The Linear Sampling Method as a Tool for "Blind" Field Intensity Shaping

Gennaro G. Bellizzi *Student Member, IEEE* and Martina T. Bevacqua *Member, IEEE*

***Abstract*—Arbitrary shaping the field intensity is a challenging problem relevant in many applications. To date, procedures addressing such a challenging problem have been developed assuming a full knowledge of both the scenario and the target. However, this is not the case in many application where the medium is only approximately known and/or modeled on the basis of some auxiliary imaging methods. In this paper, we propose a novel adaptive procedure able to shape the field intensity in an unknown (or partially unknown) scenario without the need of a quantitative scenario retrieval. The approach takes advantage from the Linear Sampling method, which belongs to the class of qualitative imaging methods, in oder to focus the field intensity with respect to different *control* points belonging to the target. Then, the desired spatial field intensity shaping is obtained by recombining the results from such single focusing problems and by exploiting an additional degree of freedom, which is represented by phase shifts of the field in the considered control points. A preliminary numerical validation and assessment is given against in-homogeneous unknown 2-D scenarios.**

***Index Terms*—Linear Sampling method; spatial field intensity shaping; support estimation; wave-field focusing.**

I. Introduction

Shaping the field intensity over an arbitrary extended target volume or focusing it in two (or more) smaller target volumes embedded into an unknown (or partially unknown) scenario is a challenging problem of intrinsic theoretical interest and also relevant in several applications. Energy harvesting [1]–[6], hyperthermia treatment planning [7], near field focusing [8], virtual and augmented reality gestural interfaces [9], [10], human posture recognition and medical rehabilitation [11], indoor navigation [12], and finally elderly and disabled people monitoring and assistance [13] are some of the most relevant applications. This problem is typically addressed determining the complex excitations coefficients feeding the antenna array of fixed geometry. So far, due to its intrinsic challenging nature, to the best of our knowledge, no strategies exist in literature directly able to arbitrary shape the field intensity within an unknown scenario.

One possibility consists in exploiting an *adaptative* procedure which could tackle the problem splitting it into three parts, as schematized in Figure 1. First, a preliminary sensing step aims at collecting information on the unknown scenario by illuminating it with known incident fields and by measuring the corresponding scattered fields. Second, geometry and electromagnetic properties of the unknown scenario, encoded in the so-called contrast function, are retrieved through an inverse scattering problem [14], [15]. This step also yields the evaluation of the total field within the domain of interest.

Third step deals with the shaping problem cast as the determination of the complex excitations "optimally" driving the antenna array by assuming the scenario to be accurately known as the second step. A very straightforward idea is that of superimposing many field intensity distributions focused in different target (say "control") points within a given target volume, as recently proposed in [16], [17]. In particular, in [17] the different coefficient sets able to focus a wave-field in the different control points have been evaluated through the well-known time reversal [18]. Then, the latter are superimposed in an "optimal" fashion by exploiting the phase shifts amongst the field at the different control points, which represent, as discussed in [17], [19], an additional degree of freedom of the problem to be optimally determined. However, performance of all the field intensity shaping approaches strictly depend on the accuracy of the reconstruction of the scenario. Unfortunately, the inverse scattering problem in the second step is a non-linear and ill-posed problem [14], [15]. The solution of such a problem is not trivial task affected by significant errors or uncertainties. moreover, most of the scattering procedures exhibit a non negligible computational burden.

In this paper, we propose an original adaptive shaping strategy which is based on the linear sampling method (LSM) [20] and is able to shape the field intensity distribution within a (partially) unknown scenario bypassing the complex retrieving step and directly going into the third step (see Figure 1). The LSM is one of the most popular and effective qualitative approaches to detect and retrieve unknown objects morphology through a simple and efficient processing of their scattered field [21]–[24]. The interesting capabilities and properties of the LSM are not limited to the above ones. Indeed, the LSM has been also physically interpreted as a tool to focus the electromagnetic field in presence of an unknown or (partially unknown) obstacle. Indeed, the LSM can provide the array complex excitation required to enforce a field which is focused in the considered target points [25].

The idea underlying the proposed blind shaping procedure has been triggered by both the physical interpretation of the LSM and the evidence that the additional degree of freedom introduced in [17], [19] (and above briefly described) yields a better control of the field intensity distribution.

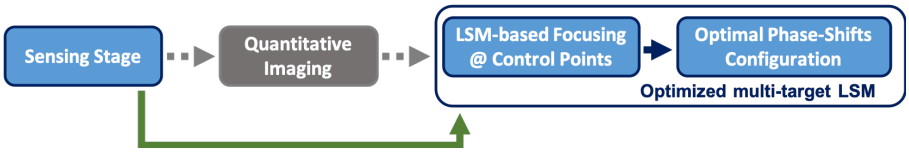

Fig. 1. Scheme of the proposed field intensity shaping methodology in unknown scenarios.

More in details, the bricks of the LSM (i.e. the excitations of the single target focusing problems and, consequently, the corresponding field induced in the scenario) are suitably combined by determining the "optimal" phase shifts configuration. The determination of this latter, which is usually based on a-posteriori observation of the shaping results, does not represent a trivial task as the total field induced in the scenario are not known. To overcome such difficulty, in this paper, the criterion yielding the "optimal" phase shifts selection, herein adopted for the first time, is based on an effective approximation of the total field, recently introduced in [26]. This latter has been derived from the physical meaning of the LSM and falls within the framework of the *virtual* scattering experiments [27], [28], as given in more details in the following sections.

Besides presenting the proposed approach, named Optimized multi-target LSM (O-mt-LSM), a preliminary numerical assessment is given. Moreover, to evaluate the actual improvements delivered by O-mt-LSM, this latter has been compared to the "simple" multi-target LSM (mt-LSM) in which the fields focused at the different control points are superimposed *in-phase*. Finally, with reference to four different 2-D homogeneous unknown scenarios, our approach have been tested to obtain: 1) a uniformly shaped distribution over a wider area; 2) a multi-spot focused distribution in two (or more) smaller target areas.

II. Focusing through The Linear Sampling Method

Let us consider a (canonical) 2-D scalar electromagnetic scattering problem and an unknown scatterer, hosted in a region under test Ω, whose cross section Σ is invariant along the z-axis. Moreover, let us suppose Ω is probed by means of N transmitting and M receiving antennas, located respectively on $\underline{r}_t$ and $\underline{r}_m$ on a closed curve Γ, polarized along the target's axis of invariance.

The LSM is one of the most famous qualitative methods to retrieve objects' support Σ from the measurements of the corresponding scattered field by solving an auxiliary linear problem [20], [22]. More in details, the LSM consists in sampling the region under test Ω into an arbitrary grid of points and solving for each point, say $\underline{r}_p$, the so-called "far field integral equation" (FFIE) as given in:

$$\sum_{t=1}^{N} \alpha_t(\underline{r}_t, \underline{r}_p) E_s(\underline{r}_t, \underline{r}_m) = G(\underline{r}_m, \underline{r}_p) \tag{1}$$

wherein α_t represents the unknown function and G is the Green's function pertaining to the background medium, i.e., the field radiated by an elementary source located in $\underline{r}_p$ and observed in $\underline{r}_m \in \Gamma$, when the targets are not present. Despite the linearity of eq. (1), the evaluation of the solution α_t is not straightforward due to the ill-posedness, so a regularization technique is required. An effective choice is that of solving it by adopting the Tikhonov regularization [24].

The estimation of the unknown support Σ is then pursued by evaluating the L_2-norm (i.e., the "energy") of the unknown function $\alpha_t(\underline{r}_t, \underline{r}_p)$, given by:

$$\Upsilon(\underline{r}_p) = \sum_{t=1}^{N} \left| \alpha_t(\underline{r}_t, \underline{r}_p) \right|^2 \tag{2}$$

The above defined indicator depends on the sampling point $\underline{r}_p$ and it turns to be bounded when the sampling point belongs to the unknown object, i.e., $\underline{r}_p \in \Sigma$, and keeps unbounded elsewhere. As a consequence, by selecting a given threshold, one can discriminate between points inside and outside the scatterers and finally retrieve Σ. Note that, in case of not connected and not convex targets, the standard LSM formulation is able to retrieve at least their convex hull. However, in order to overcome such limitations, one can take advantage from the generalized version of the FFIE [29].

Interestingly, the FFIE can be physically interpreted as an attempt to focus in each sampling point $\underline{r}_p$ the volumetric current induced by the interaction between the probing incident field and the target [24], [25]. Indeed, by solving equation (1), one is enforcing on the measurement curve a fitting between the field radiated by an elementary current in $\underline{r}_p$, namely G, and the scattered field E_s recombined according to the coefficients α_t. Note that, as one is acting on the scattered fields, by construction the radiating components of the induced currents will be focused around the selected pivot points, whereas it is not possible to foresee its non-radiating behavior. This represents a limitation of the LSM, as discussed in [24], [25].

Due to the linearity of the scattering phenomena with respect to the primary sources, the coefficients α_t can be used as complex excitations for the antenna array in order to induce currents (or equivalently total fields) focused in $\underline{r}_p \in \Omega$. More in details:

$$\mathcal{E}_{inc}(\underline{r}, \underline{r}_p) = \sum_{t=1}^{N} \alpha_t(\underline{r}_t, \underline{r}_p) E_{inc}(\underline{r}, \underline{r}_t) \tag{3}$$

is the recombined incident giving rise to the total field focused in $\underline{r}_p$, whose expression is:

$$\mathcal{E}(\underline{r}, \underline{r}_p) = \sum_{t=1}^{N} \alpha_t(\underline{r}_t, \underline{r}_p) E(\underline{r}, \underline{r}_t) \tag{4}$$

wherein $E(\underline{r}, \underline{r}_t)$ is the actual total field arising in Ω as from the sensing stage step.

Note that the LSM focuses the total field $\mathcal{E}$ in $\underline{r}_p$ while keeping under control the amplitude of the undesired side lobes which may arise only within the scatterer's support Σ. On the contrary, it does not have control outside the target support Σ [25]. On the other hand, the focusing via LSM represents an efficient procedure as the kernel of the FFIE is the same for all sampling points and the FFIE can be solved only once by processing all together the equations pertaining to the different points $\underline{r}_p$ [24].

III. The Proposed Shaping Approach

Field intensity shaping approaches generally tackle the problem by "optimally" designing the complex excitation coefficients, say I_t, feeding the antenna array surrounding Ω. In this contribution, the problem of generating an arbitrary shaped field intensity distribution in an unknown (or partially unknown) scenario is addressed. In this framework, exploiting the LSM physical interpretation, a two-steps-procedure is proposed able to shape the field intensity distribution within an arbitrary target volume $\Pi(\underline{r}) \in \Sigma$ and, at the same time, avoiding the challenging quantitative reconstruction of the scenario under test [15]. In particular, in the herein proposed approach the arbitrary shaped field intensity distribution is obtained through the superposition of different field intensity distributions focused in a set of *control points* $\underline{r}_{p_k}$ $(k = 1, .., L)$ representing a sub-group of the above introduced sampling points arbitrary located within $\Pi(\underline{r})$ [17], [19].

More in details, the proposed procedure can be summarized as it follows (see green arrow in Fig. 1):

1) *sensing stage*: the antennas surrounding Ω are exploited in order to collect information on the unknown scenario. The scenario is illuminated with known incident fields and then the corresponding scattered fields are measured.
2) *shaping stage*: this in turn is articulated in two step:
   a) *LSM-based focusing*: the FFIE underlying the LSM is solved by processing the data collected in step 1) and the evaluated α_t coefficients are exploited as complex excitation coefficients to focusing the field intensity in each single control point $\underline{r}_{p_k}$. Note, such focusing procedure only makes sense when the control points belongs to the support Σ, because of the physical interpretation of the LSM.
   b) *optimal phase shifts configuration*: the L focused field distributions as in step 2a) are conveniently superimposed, as described in the following.

Indicating with $\mathcal{E}_d(\underline{r})$ the "desired" shaped field intensity distribution, a first "basic" shaping approach, called mt-LSM, would frame the shaping problem as:

$$\mathcal{E}_d(\underline{r}) = \sum_{k=1}^{L} \mathcal{E}(\underline{r}, \underline{r}_{p_k}) \tag{5}$$

where $\mathcal{E}(\underline{r}, \underline{r}_{p_k})$ represents the field focused in the control point $\underline{r}_{p_k}$ through the LSM, as in step 2). This simply corresponds to an *in-phase* superposition of the field intensity distribution focused in the different control points. However, sub-optimal results are expected as not all the degrees of freedom of the problem are exploited [17], [19].

Let us introduce an auxiliary variable, say $\phi_k \in [0, 2\pi]$, having the physical meaning of the phase shift between the fields in the control point $\underline{r}_{p_1}$ and $\underline{r}_{p_k}$. For each (sampled) value of auxiliary variables ϕ_k, the proposed O-mt-LSM approach casts the shaping problem as the combination of the fields focused through the LSM in correspondence of $\underline{r}_{p_k}$ as:

$$\mathcal{E}_d(\underline{r}) = \sum_{k=1}^{L} \mathcal{E}(\underline{r}, \underline{r}_{p_k}) e^{j\phi_k} \tag{6}$$

where ϕ_k is an additional degree of freedom of the problem[1] to be optimally determined within the range $[0, 2\pi]$. Such field intensity distribution can be achieved when the array is fed by the complex excitation coefficients, I_t, as in:

$$I_t(\underline{r}_t) = \sum_{k=1}^{L} \alpha_t(\underline{r}_t, \underline{r}_{p_k}) e^{j\phi_k} \tag{7}$$

When dealing with more control points, the shaping problem is cast as the determination of the phase shifts configuration delivering some optimality of the overall shaped field distribution, i.e., $\mathcal{E}_d(\underline{r})$. Note, in case L control points are considered, the phase shift configuration is represented by the vector $\underline{\phi} = \{\phi_k\}_{k=1,..,L}$ containing the L auxiliary variables representing the phase shift between the field at the reference control point $\underline{r}_{p_1}$ and the *k-th* control point.

Finally, note that, both in equations (5) and (7) the total fields $\mathcal{E}_d(\underline{r})$ focused in the control points are not known as we are dealing with a blind shaping problem.

IV. The Optimal $\underline{\phi}$ in Unknown Scenarios

A crucial role in the proposed approach, as well as in [17], [19], is represented by the determination of the optimal phase shifts configuration. Hence, the definition of an objective function and the application of some optimization criterion is needed. In this work we have intuitively selected the average field intensity in the target volume, say $\int_{\Pi(\underline{r})} |\mathcal{E}_d(\underline{r})|^2$, as cost function to be maximized. However, the evalutation of this cost function would require a quantitative knowledge of the scenario. As a consequence, such an optimization problem is prevented by the impossibility of knowing the total fields $\mathcal{E}(\underline{r}, \underline{r}_{p_k})$ inside the region under test. Fortunately, the LSM has been recently exploited to introduce an original and effective approximation of the total fields [26]. This latter has directly been derived both from the FFIE's physical interpretation and the framework of the *virtual* scatering experiments [27], [28].

More in details, the LSM-based total fields approximation reads as follows:

$$\widehat{\mathcal{E}}(\underline{r}, \underline{r}_{pk}) = \mathcal{E}_{inc}(\underline{r}, \underline{r}_{pk}) + LP\{G(\underline{r}, \underline{r}_{pk})\} \tag{8}$$

wherein the second addendum is the low pass filtered version of the elementary field having singularity in the origin of the sampling point, as disccused in [26]. The total field approximation in (8) states that the total field arising in eq. (4) can be approximated as the contribution of the recombined original field according to eq. (3) plus the filtered version

[1] Notably, $\phi_1 = 0$

TABLE I
PARAMETERS FOR THE TESTED NUMERICAL CONFIGURATIONS.

Configuration	L	N_{TX}	r_o	l_Ω	mesh grid
I	2	16	$1.6\lambda_b$	$1.6\lambda_b$	64×64
II	3	16	$1.6\lambda_b$	$1.6\lambda_b$	64×64
III	2	18	$4\lambda_b$	$4\lambda_b$	64×64
IV	3	26	$4\lambda_b$	$4\lambda_b$	50×50

of the field pattern radiating in Ω by an elementary current located in $\underline{r}_{pk}$. Further details are repoted in [26].

As a consequence, the optimization problem for the selection of the optimal $\underline{\phi}$ can be re-cast as:

$$\underset{\underline{\phi}}{\text{argmax}} \int_{\Pi(\underline{r})} \left|\widehat{\mathcal{E}}_d(\underline{r})\right|^2 \tag{9}$$

subject to:

$$\widehat{\mathcal{E}}_d = \sum_{k=1}^{L} \widehat{\mathcal{E}}(\underline{r}) e^{j\phi_k} \tag{10}$$

Obviously, the optimization outcome depends on the quality of the approximation in eq. (8).

When just a few control points are of interest, the optimal solution can be determined in an enumerative fashion observing a-posteriori the different $\underline{\phi}$-solutions and picking the most convenient solution according to the adopted and most suitable cost function for the application at hand. Notably, dealing with L control points and M sampled values of the auxiliary variables in $[0, 2\pi]$ will require M^{P-1} linear superposition, thus impacting the computational time. As a consequence, when considering more control points and finer sampling grids for the auxiliary variable, parallel computing can be exploited as well as more sophisticated optimization strategies are required. Hereto, the optimization problem (9)-(10) has been tackled in an enumerative fashion since our main aim is that of demonstrating the usefulness of the introduced additional degree of freedom and testing it in the hard task of shaping the field intensity in unknown scenarios. Present efforts are aimed at designing alternatives fruitful procedures addressing such a need.

V. VALIDATION RESULTS AND DISCUSSION

Performance and limitations of the proposed approach have been tested over 4 different scenarios and two different shaping configurations. In particular, two of them concern with the generation of a uniformly shaped field intensity distribution exploiting respectively two and three control points, say configuration **I** and **II**. On the other hand, the last two configurations deal with the generation of a multi-spot focused field intensity distribution exploiting again two and three control points, say configuration **III** and **IV** respectively.

In our numerical analysis we supposed the unknown target embedded into a square region Ω with permittivity $\epsilon_b = 1$, conductivity $\sigma_b = 0$ and side l_Ω surrounded by a circular array of antennas, of radius r_o. Such an array is both able to probe Ω in the sensing stage and to radiate the fields during the shaping stage. In particular in the sensing stage such array is fed with unit amplitude currents and a multiview-multistatic configuration is exploited [24]. The array is supposed to be

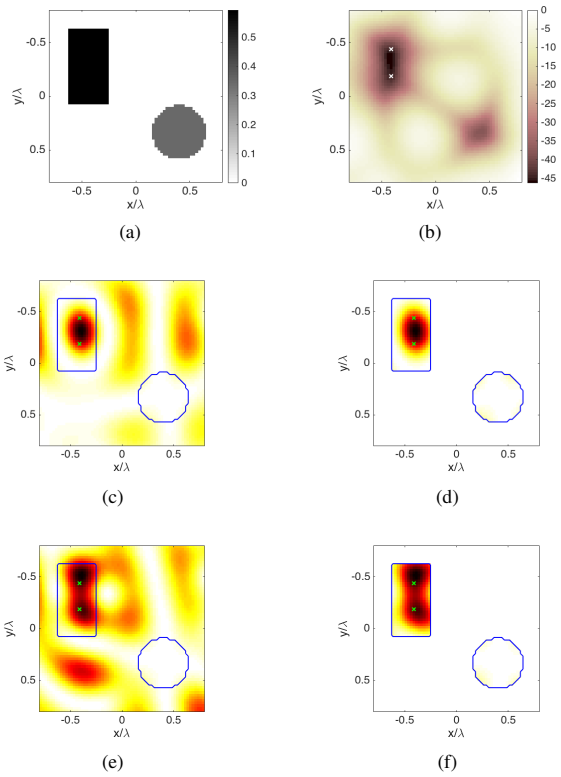

Fig. 2. Contrast function (a) and normalized LSM indicator map in logarithmic scale (b) for configuration **I**. The Normalized squared field amplitudes achieved by means of mt-LSM and O-mt-LSM are respectively depicted within the whole domain of investigation, (c) and (e) respectively, and thresholded to the actual support of the unknown objects, (d) and (f) respectively. Control points are marked as *"x"*.

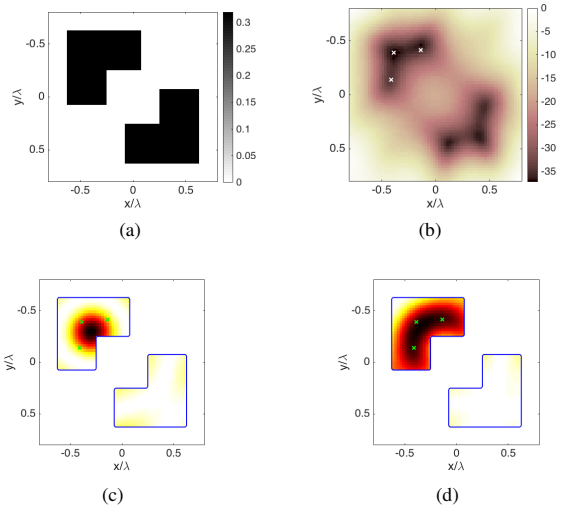

Fig. 3. Contrast function (a) and normalized LSM indicator map in logarithmic scale (b) for configuration **II**. The normalized thresholded squared field amplitudes achieved by means of mt-LSM and O-mt-LSM are respectively depicted (c) and (d). Control points are marked as *"x"*.

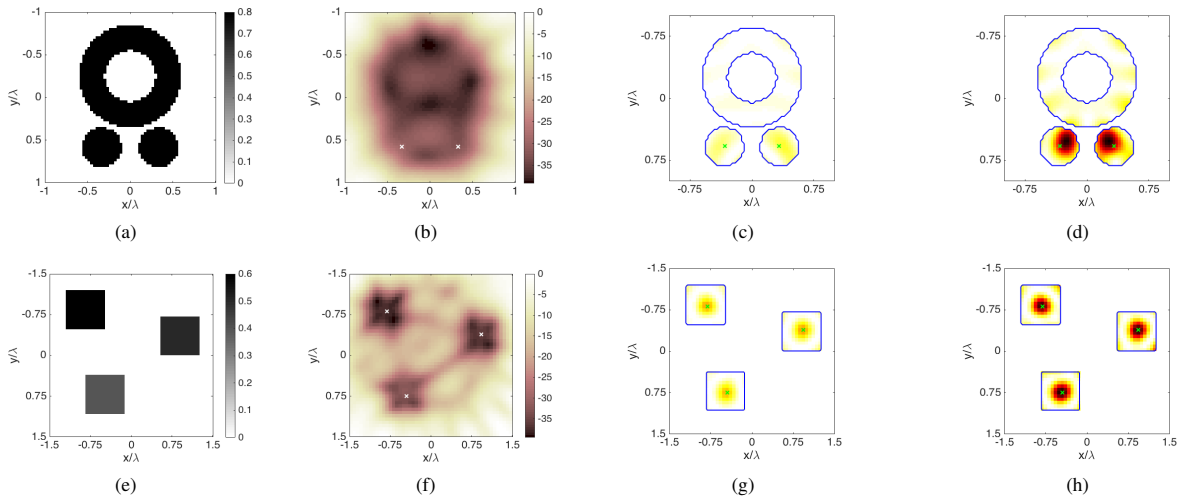

Fig. 4. Contrast functions (a)-(d) and normalized LSM indicator map in logarithmic scale (b)-(e) for configurations **III** and **IV** respectively. The normalized thresholded squared field amplitudes achieved by means of mt-LSM and O-mt-LSM are respectively depicted in (c) and (d) for configuration **III** and in (g) and (h) for configuration **IV**. Control points are marked as *"x"*.

embedded into the background medium, while the number of antenna elements N_{TX} has been determined in a non-redundant way as well as to provide a non super-directive arrays. In particular, according to [30], $N_{TX} \approx 2k_b a$, where k_b is the wavenumber in the host medium and a the radius of the minimum circle enclosing the investigated scenario. Table I reports the specific parameters values adopted.

Before presenting the validating results, let us again stress that because of the LSM physical interpretation, the shaping has a meaning only when $\underline{r}_{pk} \in \Sigma$. Hence, the target area and the control points selection has been pursued only after the identification of the target support Σ through the LSM indicator map (see eq. (2)). In the following, according to [17], [19], [31], the target area $\Pi(\underline{r})$ has been indicated as the superposition of spheres of radius $\approx \lambda_b/4$[2] centered at $\underline{r}_{pk}$. Quantitative performance evaluation have been pursued exploiting the coverage factor (CF) as a quality metric. TC has been defined as the fraction of $\Pi(\underline{r})$ in which the squared amplitude of the field is higher than the 25% of its maximum value[3].

In order to understand the effective role of the auxiliary parameters $\underline{\phi}$ and of the adopted cost function, a first result against configuration **I** is reported in Fig. 2. Fig. 2.(a) and (b) depict the scenario and its inherent qualitative reconstruction through LSM, wherein the exploited two control points are marked as white crosses. In order to visually enlighten the crucial role played by the introduced degrees of freedom, i.e., $\underline{\phi}$, the normalized squared amplitudes of the fields obtained through both mt-LSM (Fig.s 2.(c)-(d)) and O-mt-LSM (Fig.s 2.(e)-(f)) have been reported. For this first example, the CF passed from 39% to 77% when the proposed approach is exploited. Finally, to validate the appropriateness of the adopted cost function, both the normalized squared amplitude of the fields over the whole domain of interest, i.e., Ω, and its version thresholded to the actual true support of the hosted objects are reported in figure 2. This clearly shows the impossibility of the LSM in controlling the field intensity distribution outside the target support, alike also other focusing/shaping approaches [17], [18].

Then, the proposed approach has been tested to achieve a wider uniformly shaped field intensity with an arbitrary shape. The normalized squared amplitudes of the field intensities distributions obtained by means of both mt-LSM and O-mt-LSM for configuration **II** are depicted in Fig. 3. In this configuration an *L-shaped* field intensity distribution is achieved by means of three control points. Note that the CF increases from 33% to 90% when exploiting the O-mt-LSM, while the not-optimized mt-LSM completely fails.

Lastly, as far as the possibility to achieve multi-spot shaped field intensities is concerned, Fig. 4 depicts the normalized squared amplitudes of the fields obtained by means of both mt-LSM and O-mt-LSM for configurations **III** and **IV**. In these latter configurations, respectively two and three control points have been exploited. When exploiting the O-mt-LSM, the CF increases from 0% [4] to 60% for configuration **III** and from 26% to 71% for configuration **IV**. Again, let us note that the not-optimized mt-LSM completely fails in achieving the desired multi-spot field intensity distribution.

VI. Conclusions

In this work, for the first time we proposed an approach for *blind* shaping, i.e. able to arbitrary shape the field intensity distribution into a (partially) unknown scenario without the need of quantitative retrieving the electromagnetic properties of the targets herein embedded. Starting from the LSM physical interpretation as a tool to focus the electromagnetic field

[2] λ_b being the wavelength in the host medium

[3] Ideally, CF=1.

[4] This value means that the amplitude of the field is not higher than the 25% of its maximum value, which unfortunately occours outside the support of the targets.

intensity in presence of unknown obstacles, a novel approach is proposed which takes advantage from considering single focusing problem as well as additional degrees of freedom, surprisingly neglected so far, that are the phase shifts of the field in the considered control points.

While the computational time of the proposed approach is very limited and advantageous as compared to other more cumbersome approaches, two main limitations(/cons) are affecting the proposed technique. First, the limitations of the technique are related to the ones of the LSM [24]. As a consequence, the herein proposed blind shaping procedure woks fine as long as the LSM is able to focus the field intensity in the selected control points. Moreover, the approach is able to shape a wave-field only over a target area belonging to the unknown obstacles. This could not represent a strict limitation as one is interested in shaping the field intensity distributions only within the detected unknown objects. On the other hand, the LSM can be easily extended to the case of non homogeneous scenario and, hence, the proposed approach can be applied when an approximated a priori knowledge of the scenario of interest is available. Second, determining the optimal phase shifts configuration represents a case-specific, challenging and open problem. Driven by the assumption that the LSM has only control within the scatterers support, in this work the average value of the squared amplitude of the field into the detected target area has been chosen as cost function to be maximized. Moreover, a selection criterion based on a recently introduced total field approximation has been adopted [26]. Then, the determination of the optimal phase shifts configuration is robust as long as the approximated total field within the domain Ω is close to the actual one. This depends on the validity range of the adopted VE-based approximation [26].

Present efforts are aimed at devising novel selection criterion as well as optimization strategies for the optimal phase shift selection and at exploiting the proposed procedure within a real 3-D application scenario.

ACKNOWLEDGMENTS

The authors want to thank Prof. Tommaso Isernia for the fruitful discussions, which inspired the writing of this paper.

REFERENCES

[1] C. Hsi-Tseng, H. Tso-Ming, W. Nan-Nan, C. Hsi-Hsir, T. Chia, and P. Nepa, "Design of a near-field focused reflectarray antenna for 2.4 GHz RFID reader applications," *IEEE Trans. Ant. Prop.*, vol. 59, no. 3, pp. 1013–1018, 2011.

[2] M. Merenda, I. Farris, C. Felini, L. Militano, S. C. Spinella, F. G. D. Corte, and A. Iera, "Performance Assessment of an Enhanced RFID Sensor Tag for Long-run Sensing Applications," *IEEE SENSORS*, 2014.

[3] Z. Zou, A. Gidmark, T. Charalambous, and M. Johansson, "Optimal radio frequency energy harvesting with limited energy arrival knowledge," *IEEE Journal on Selected Areas in Communications*, vol. 34, pp. 3528–3539, Dec. 2016.

[4] L. Elmorshedy, C. Leung, and S. A. Mousavifar, "RF energy harvesting in df relay networks in the presence of an interfering signal," in *Proc. IEEE Int. Conf. Communications (ICC)*, pp. 1–6, May 2016.

[5] A. Alsharoa, A. Celik, and A. E. Kamal, "Energy harvesting in heterogeneous networks with hybrid powered communication systems," in *Proc. IEEE 86th Vehicular Technology Conf. (VTC-Fall)*, pp. 1–5, Sept. 2017.

[6] M. Merenda, C. Felini, and F. G. D. Corte, "An autonomous and energy efficient smart sensor platform," in *Proc. IEEE SENSORS*, pp. 1208–1211, Nov. 2014.

[7] M. M. Paulides, G. M. Verduijn, and N. V. Holthe, "Status quo and directions in deep head and neck hyperthermia," *Radiation Oncology (2016) 11:21*, 2016, DOI 10.1186/s13014-016-0588-8.

[8] I. Iliopoulos and et al., "3D near-field shaping of a focused aperture," in *Antennas and Propagation (EuCAP), 2016 10th European Conference on, DOI: 10.1109/EuCAP.2016.7481747*, 2016.

[9] R. J. Przybyla, H. Tang, S. E. Shelton, D. A. Horsley, and B. E. Boser, "12.1 3D ultrasonic gesture recognition," in *Proc. IEEE Int. Solid-State Circuits Conf. Digest of Technical Papers (ISSCC)*, pp. 210–211, Feb. 2014.

[10] R. Carotenuto, R. Ionescu, P. Tripodi, and F. Urbani, "Three dimensional ultrasound gestural interface," in *Proc. IEEE Int. Ultrasonics Symp*, pp. 690–693, Sept. 2009.

[11] Y. Ebisawa, "A pilot study on ultrasonic sensor-based measurement of head movement," *IEEE Transactions on Instrumentation and Measurement*, vol. 51, pp. 1109–1115, Oct. 2002.

[12] J. Torres-Solis, T. H. Falk, and T. Chau, "A review of indoor localization technologies: towards navigational assistance for topographical disorientation," in *Ambient Intelligence*, InTech, 2010.

[13] A. Marco, R. Casas, J. Falco, H. Gracia, J. I. Artigas, and A. Roy, "Location-based services for elderly and disabled people," *Computer communications*, vol. 31, no. 6, pp. 1055–1066, 2008.

[14] M. Bertero and P. Boccacci, *Introduction to Inverse Problems in Imaging*. Inst. Phys., Bristol, U.K., 1998.

[15] D. Colton and R. Kress, *Inverse acoustic and electromagnetic scattering theory*. 2nd ed Springer, Berlin, 1998.

[16] D. Zhao and M. Zhu, "Generating Microwave Spatial Fields with Arbitrary Patterns," *IEEE Antennas and Wireless Propagation Letters*, no. 99, pp. 1–4, 2016.

[17] G. G. Bellizzi, M. T. Bevacqua, L. Crocco, and T. Isernia, "Optimized multi-target time reversal for 3-D field intensity shaping," *IEEE Transactions on Antennas and Propagation*, p. 1, 2018.

[18] M. Fink, "Time reversal of ultrasonic fields. i. basic principles," *IEEE Trans. Ultrason. Ferroelectr. Freq. Control.*, vol. 39, pp. 555–566, 1992.

[19] G. G. Bellizzi, D. A. M. Iero, L. Crocco, and T. Isernia, "Three-dimensional field intensity shaping: The scalar case," *IEEE Antennas and Wireless Propagation Letters*, vol. 17, pp. 360–363, Mar. 2018.

[20] D. Colton, H. Haddar, and M. Piana, "The linear sampling method in inverse electromagnetic scattering theory," *Inverse Probl.*, vol. 19, pp. 105–137, 2003.

[21] F. Cakoni and D. Colton, "The linear sampling method for cracks," *Inverse problems*, vol. 19, no. 2, p. 279, 2003.

[22] F. Cakoni and D. Colton, *Qualitative methods in inverse scattering theory: An introduction*. Springer Science & Business Media, 2005.

[23] M. Akıncı, T. Çağlayan, S. Özgür, U. Alkaşı, M. Abbak, and M. Çayören, "Experimental assessment of linear sampling and factorization methods for microwave imaging of concealed targets," *International Journal of Antennas and Propagation*, vol. 2015, 2015.

[24] I. Catapano, L. Crocco, and T. Isernia, "On simple methods for shape reconstruction of unknown scatterers," *IEEE Transactions on Antennas and Propagation*, vol. 55, no. 5, pp. 1431–1436, 2007.

[25] L. Crocco, L. Di Donato, D. A. Iero, and T. Isernia, "An adaptive method to focusing in an unknown scenario," *Progress In Electromagnetics Research*, vol. 130, pp. 563–579, 2012.

[26] L. Crocco, I. Catapano, L. D. Donato, and T. Isernia, "The linear sampling method as a way to quantitative inverse scattering," *IEEE Transactions on Antennas and Propagation*, vol. 60, pp. 1844–1853, Apr. 2012.

[27] L. D. Donato, M. Bevacqua, T. Isernia, I. Catapano, and L. Crocco, "Improved quantitative microwave tomography by exploiting the physical meaning of the linear sampling method," in *Proc. 5th European Conf. Antennas and Propagation (EUCAP)*, pp. 3828–3831, Apr. 2011.

[28] M. T. Bevacqua, L. Crocco, L. Di Donato, and T. Isernia, "An algebraic solution method for nonlinear inverse scattering," *IEEE Transactions on Antennas and Propagation*, vol. 63, no. 2, pp. 601–610, 2015.

[29] L. Crocco, L. Di Donato, I. Catapano, and T. Isernia, "An improved simple method for imaging the shape of complex targets," *IEEE Transactions on Antennas and Propagation*, vol. 61, no. 2, pp. 843–851, 2013.

[30] O. M. Bucci and T. Isernia, "Electromagnetic inverse scattering: retrievable information and measurement strategies," *Radio Sci.*, vol. 32, pp. 2123–2137, 1997.

[31] O. Bucci and G. Franceschetti, "On the degrees of freedom of scattered fields," *IEEE Trans. Antennas Propag.*, vol. 37, pp. 918–926, 1989.